

# Structural, Thermal and Electrical Studies of $\text{Al}_2\text{O}_3$ Nanoparticle Soaked Electrolyte Gel Films for Novel Proton Conducting ( $\text{H}^+$ ion) Eco-friendly Device Applications

Neelesh Rai, Chandra Prakash Singh, Lovely Ranjta \*

Department of Physics, AKS University, Satna, India

## Email address:

neeshsssi@gmail.com (N. Rai), cpsingh4071@gmail.com (C. P. Singh), lovelyranjta@gmail.com (L. Ranjta)

\*Corresponding author

## To cite this article:

Neelesh Rai, Chandra Prakash Singh, Lovely Ranjta. Structural, Thermal and Electrical Studies of  $\text{Al}_2\text{O}_3$  Nanoparticle Soaked Electrolyte Gel Films for Novel Proton Conducting ( $\text{H}^+$  ion) Eco-friendly Device Applications. *American Journal of Nano Research and Applications*. Vol. 10, No. 1, 2022, pp. 1-8. doi: 10.11648/j.nano.20221001.11

Received: April 20, 2022; Accepted: May 10, 2022; Published: May 31, 2022

**Abstract:** An attempt has been made to prepare and characterize ammonium acetate ( $\text{NH}_4\text{CH}_3\text{COO}$ ) salt and Aluminium Oxide ( $\text{Al}_2\text{O}_3$ )-soaked polyvinyl alcohol (PVA) based [ $\text{PVA-NH}_4\text{CH}_3\text{COO}:\times\text{wt}\%\text{Al}_2\text{O}_3$ ] system nanocomposite polymer gel electrolyte (NCPGE) films using a solution cast technique. The SEM and XRD studies revealed improvement in amorphous nature. The degree of crystallinity and average crystallite size of electrolytes with respect to  $\text{Al}_2\text{O}_3$  were projected to ascertain improvement in amorphous nature. FTIR studies confirmed the complexation between PVA,  $\text{NH}_4\text{CH}_3\text{COO}$  and  $\text{Al}_2\text{O}_3$ . The DSC studies show better thermal response upon addition of  $\text{Al}_2\text{O}_3$  nanofiller. TGA studies reveal the mass of nanocomposite polymer gel electrolyte decreases continuously with increase in the  $\text{Al}_2\text{O}_3$  nanofiller contents. Closer assessment of conductivity behavior shows two maximas: one around 0.5wt% and the other around 1wt% filler concentration which is a typical feature for nanocomposite gel polymer electrolytes. The temperature dependence of electrical conductivity shows a combination of Arrhenius and Vogel–Tamman–Fulcher (VTF) behavior. The ionic conductivity is found to increase with addition of filler concentration and optimum ionic conductivity of  $3.88\times10^{-4}\text{ Scm}^{-1}$  with wide electrochemical stability of  $\pm4.78\text{V}$  is achieved at 1wt%  $\text{Al}_2\text{O}_3$  nano filler and confirms the availability of  $\text{H}^+$  ion (proton) in the system suitable for the development of environment friendly rechargeable batteries application.

**Keywords:** XRD, DSC, Conductivity, Nanocomposite Polymer Gel Electrolytes, Proton-Conducting Batteries

## 1. Introduction

Ion conducting behavior of polymer electrolytes is one such property which has been intensively and extensively studied in recent years for device applications [1, 2]. The ionic conductivity is most intensively studied category of polymer electrolytes i.e. solvent free polymer electrolyte; is usually limited by segmental mobility and concentration of charge carriers though these electrolyte systems possess good mechanical integrity [3-5]. Various techniques have been reported in recent years to enhance ion conduction and mechanical properties of these polymer electrolytes [6, 7]. Since high ionic conductivity is eagerly understood due to presence of liquid phase which still provides liquid like channel in gel system. However, several recent studies

dealing with polar polymers, have gained different insight to the role of polymer matrix. Within the umbrella of polymer gel electrolytes, PVA is also one of the prominent polymer because of its good solvent holding capability and wide temperature window [8].

In order to achieve better thermal and electrochemical stability under ambient conditions such as synthesized gel electrolytes are usually doped with either a high molecular weight polymer leading to formation of blend based electrolyte [9] or inorganic inert filler [10, 11] leading to formation of composite polymer gel electrolyte. Similar approach has been attempted in the present work to improve the performance of  $\text{PVA-NH}_4\text{CH}_3\text{COO}$  electrolytes by dispersal of nano sized  $\text{Al}_2\text{O}_3$  filler particles. This system is expected to significantly obstruct crystallization progression

in polymer based nanocomposite electrolytes and thus improve ionic conductivity, thermal stability as well as its electrochemical stability for long term use in eco-friendly electrochemical devices particularly batteries and smart windows owing to possibility of single ion conduction. Free standing NCPGE films were prepared by conventional solution cast technique and subsequently characterized by structural, thermal, electrochemical and electrical conductivity measurements.

## 2. Experimental Analysis

In this study, polymer PVA (average molecular weight 124,000–186,000 Aldrich make) was used for supporting gel matrix, salt ammonium acetate ( $\text{NH}_4\text{CH}_3\text{COO}$ ), AR grade sd. fine chem. make for developing proton conducting gel electrolyte and aprotic solvent dimethyl sulphoxide (DMSO) Merk limited, Mumbai make were chosen for synthesis of composite electrolyte system.  $\text{Al}_2\text{O}_3$  nano particles used in this study was obtained from Alfa Aesar, CAS Number: 1344-28-1 possessing average particle size 40-50nm.

For formation of stable gel films, PVA: $\text{NH}_4\text{CH}_3\text{COO}$  based proton conducting gel electrolyte, PVA was dispersed in 1 mole salt solution of  $\text{NH}_4\text{CH}_3\text{COO}$  in DMSO in different stoichiometric ratios to form pristine gel electrolyte (PVA: $\text{NH}_4\text{CH}_3\text{COO}$  system). Composite polymer gel electrolytes were prepared by adding  $\text{Al}_2\text{O}_3$  nano particles in pristine gel electrolyte solution in different weight proportions followed by thorough mixing at slightly elevated temperature on a magnetic stirrer.

Synthesised polymer nanocomposite gel electrolytes of [PVA- $\text{NH}_4\text{CH}_3\text{COO}$ :xwt% $\text{Al}_2\text{O}_3$ ] have been characterized with the help of different experimental probes to assess their performance for device application.

Structural morphology, complexation and crystal size of different polymer nanocomposite electrolytes were studied by X-ray Diffractometer (D2 Phaser model: 08 discover, Bruker). The surface morphology of the electrolyte films was observed using a JEOL scanning electron microscope (Model JSM-6390A). FTIR spectrums were done by Bruker Alpha platinum ATR Spectrophotometer having range 4,000-600  $\text{cm}^{-1}$  at room temperature for understanding the interaction among the present constituents.

To understand thermal response of the composite electrolytes, differential scanning calorimetry (DSC) scans were carried out on a NETZSCH DSC model STA449F1 in the temperature range RT to 340°C at a heating rate 5°C/min. under nitrogen atmosphere.

Cyclic Voltammetry (CV) and Linear Sweep voltammetry (LSV) measurements were taken by using an Electrochemical Analyzer (CH Instruments, USA make; CHI608D) in the  $\pm 3\text{V}$  sweep range with the scan rate at  $0.1\text{Vs}^{-1}$  to examine the electrochemical stability and better performance in window and also to confirm the presence of proton ion present in the gel membranes. Complex-impedance spectra were also performed from 1Hz–1MHz frequency range at different temperatures from 30°C–95°C.

## 3. Results and Discussion

### 3.1. Scanning Electron Microscopy Studies

Figure 1(a-d) depicts the surface morphology of Pure  $\text{Al}_2\text{O}_3$  nano powder and  $\text{NH}_4\text{CH}_3\text{COO}$ : PVA electrolyte films containing 0, 0.5 and 1.0 wt% concentration of  $\text{Al}_2\text{O}_3$ . SEM Image of unfilled PVA gel electrolyte shows a closed spongy structure made up of PVA chains (figure 1b). Addition of 0.5 wt%  $\text{Al}_2\text{O}_3$  nano particles decreases the porosity of PVA composite electrolyte because  $\text{Al}_2\text{O}_3$  nano particles are stuck in between the chains (figure 1c).  $\text{Al}_2\text{O}_3$  nano filler particles are not completely riveted as shown by white spots in the SEM image. On addition of 1 wt%  $\text{Al}_2\text{O}_3$  nano particles (figure 1d), chains of PVA are completely covered with  $\text{Al}_2\text{O}_3$  nano particles. This shows complete dispersion of  $\text{Al}_2\text{O}_3$  nanofiller in electrolyte film. On further addition of  $\text{Al}_2\text{O}_3$  nano particles in the system, separate grains comprising of  $\text{Al}_2\text{O}_3$  nano particles and PVA electrolyte are formed. Partially crystalline texture is confirmed due to irregular size and shape of the grains. The images provide heterogeneity in the phase of nanocomposite electrolyte system.

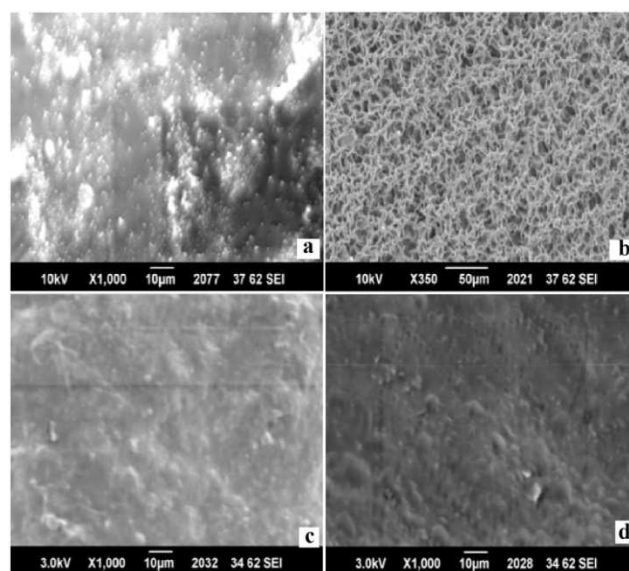


**Figure 1.** SEM images of (a) pure  $\text{Al}_2\text{O}_3$  (b) 0 wt% (c) 0.5 wt% (d) 1.0 wt% addition of  $\text{Al}_2\text{O}_3$  nanoparticles in NCPGE membranes.

### 3.2. X-ray Diffraction Studies

The XRD patterns of polymer gel electrolyte films of  $\text{NH}_4\text{CH}_3\text{COO}$ : PVA without and with  $\text{Al}_2\text{O}_3$  nanofillers are shown in figures 2(a-e). The XRD pattern ‘inset diffractogram’ comprises of crystalline strong peaks of pure  $\text{Al}_2\text{O}_3$  at  $2\theta = 28.7^\circ$  (102),  $32.5^\circ$  (213),  $36.6^\circ$  (311),  $38.3^\circ$  (006),  $39.9^\circ$  (223),  $45.7180^\circ$  (040),  $67.2^\circ$  (046) crystal planes reflecting pure crystalline structure. Comparison of this XRD data with JSPDS data reveals orthorhombic structure and lattice parameters  $a=7.934\text{\AA}$ ,  $b=7.956\text{\AA}$ ,  $c=11.71\text{\AA}$  have been calculated [7, 12]. In diffraction pattern of DMSO casted PVA gel film (curve c), apart from background modulation, two relatively intense peaks at  $19.6^\circ$  and  $20.2^\circ$

with combined broadening appear and correspond to characteristics peak of polycrystalline PVA-DMSO complex [13]. The XRD pattern for [PVA-NH<sub>4</sub>CH<sub>3</sub>COO:×wt% Al<sub>2</sub>O<sub>3</sub>] film exhibits shifting of PVA related peak (around 20° in PVA: DMSO gel film) towards lower 2θ value (18.5°) on addition of salt NH<sub>4</sub>CH<sub>3</sub>COO in PVA matrix (pattern b). Upon addition of 0.2 wt% Al<sub>2</sub>O<sub>3</sub> nanofiller, the peak broadens up and shifts toward lower 2θ values (pattern c). This broadened peak might be related to [PVA-NH<sub>4</sub>CH<sub>3</sub>COO:×wt%Al<sub>2</sub>O<sub>3</sub>] complex appears on account of interaction of electrolyte with Al<sub>2</sub>O<sub>3</sub> leading to formation of nanocomposite as this doesn't correspond to any of the pristine materials PVA, Al<sub>2</sub>O<sub>3</sub>, and NH<sub>4</sub>CH<sub>3</sub>COO. Further this broadened peak shifts further on toward lower 2θ values (pattern c-e) on increase of Al<sub>2</sub>O<sub>3</sub> content upto 1.0wt% in NCPGE which reflects complete absorption of Al<sub>2</sub>O<sub>3</sub> particles in the PVA matrix/enhanced intercalation of dispersoids in matrix electrolyte. This feature ascertains improvement in system morphology.

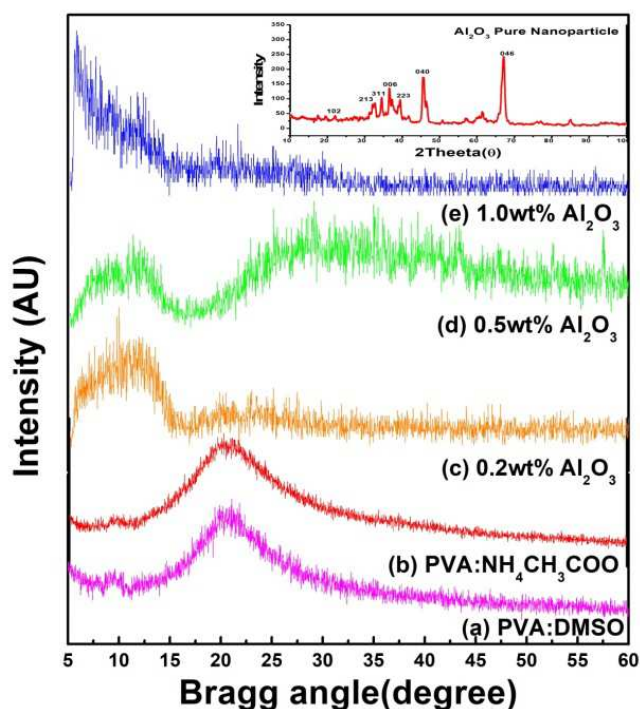


**Figure 2.** X-Ray Diffractograms for (a) PVA-DMSO (b) PVA-NH<sub>4</sub>CH<sub>3</sub>COO, (c) 0.2 wt% (d) 0.5 wt% (e) 1.0 wt% addition of Al<sub>2</sub>O<sub>3</sub> nanoparticles in NCPGEs. Inset image represents the X-Ray diffractogram of pure Al<sub>2</sub>O<sub>3</sub> nanoparticles.

Degree of crystallinity (Xc) of electrolytes with respect to Al<sub>2</sub>O<sub>3</sub> was estimated to ascertain improvement in amorphous nature [7, 12] presuming filler to be fully crystalline (table 1) and observed that it decreases with increase in filler concentration which again ascertains change in system morphology on addition of filler. Likewise average crystallite size in composite system (table 1) was also estimated using well known Debye Scherrer's relation to ensure nanodimension of resulting system after dispersed of filler particles [12].

**Table 1.** Average crystallites size, crystallinity and ionic transference number of nanocomposite polymer gel electrolyte [PVA-NH<sub>4</sub>CH<sub>3</sub>COO:×wt% Al<sub>2</sub>O<sub>3</sub>] system.

Al <sub>2</sub> O <sub>3</sub> contents	Average crystallites size (nm)	Crystallinity Xc (%)	Ionic transference Number t <sub>ion</sub>
0 wt%	~ 45	64.3	0.93
0.2 wt %	~41	43.4	0.96
0.5 wt%	~ 33	32.6	0.96
1.0 wt%	~ 29	31.4	0.98

Interestingly, it is observed that average crystallite size decreases with increasing filler content till 1wt% thereafter it increases. This is due to interaction between the outer layers of materials and filler, which reduces the crystallite size of the filler. This behavior can also be correlated to Tsagaropoulos model [14]. These observations are well supported with SEM investigations discussed above.

### 3.3. Infrared (IR) Spectroscopy Studies

It is strongly believed that effects like ion polymer interaction, ion solvation and matrix behavior are important factor to understand the conductivity behavior of gel electrolytes. IR studies have been found to be useful experimental tool to understand structure-property correlations in gel electrolyte investigation [15]. Thus IR spectra were recorded for polymer gel electrolyte and corresponding polymer nanocomposite electrolytes to understand interaction between various components and their complexation behavior.

Figure 3(a) depict the IR spectra for pristine and its composite figure 3(c-g) in transmittance mode and table 2 shows the transmittance peaks with possible assignments. IR spectra of PVA and DMSO in figure 3(c) gives the presence of another absorption peaks at wave numbers 702, 1362, 1375, 1418cm<sup>-1</sup> which are absent in spectra which is related to pure PVA in figure 3(a) and DMSO showing strong interaction among components and resulting in the formation of PVA:DMSO complex [13]. Shift of 702, 843, 1436, 1643 and 2939cm<sup>-1</sup> peaks towards higher wave number up on addition of NH<sub>4</sub>CH<sub>3</sub>COO (figure 3d) due to interaction with PVA-DMSO reflects the formation of PVA:NH<sub>4</sub>CH<sub>3</sub>COO-DMSO figure 3(d).

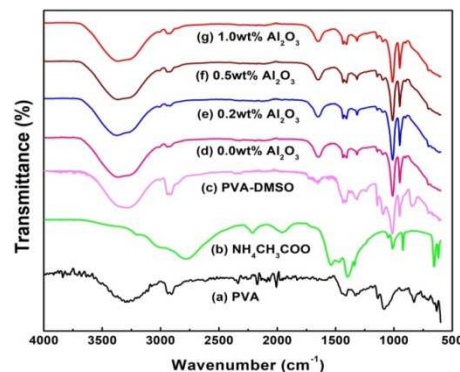


**Figure 3.** FTIR spectra of (a) pure PVA (b) NH<sub>4</sub>CH<sub>3</sub>COO (c) PVA-DMSO (d) NCPGE membranes of [PVA-NH<sub>4</sub>CH<sub>3</sub>COO:×wt%Al<sub>2</sub>O<sub>3</sub>] system containing 0 wt% (e) 0.2 wt%, (f) 0.5 wt% (g) 1.0 wt% concentrations of Al<sub>2</sub>O<sub>3</sub> nanoparticles.

The broad absorption peak from 500 to 800cm<sup>-1</sup> in FTIR spectra of pure Al<sub>2</sub>O<sub>3</sub> is attributed to the characteristic transmittance band of Al<sub>2</sub>O<sub>3</sub> reported by Ghezelbash et al [16]. Besides existence of absorption peaks at 1628, 1385 and 1124 cm<sup>-1</sup> also corresponds to characteristic band frequencies of Al<sub>2</sub>O<sub>3</sub>, which are not present in the spectra related to [PVA-NH<sub>4</sub>CH<sub>3</sub>COO:×wt% Al<sub>2</sub>O<sub>3</sub>] NCPGE in figure 3(e-g) reflecting strong interactions of Al<sub>2</sub>O<sub>3</sub> with pristine electrolyte. Shifting of the characteristic peak of pristine electrolytes observed from 3372cm<sup>-1</sup> to 3349cm<sup>-1</sup> which indicates intercalation of Al<sub>2</sub>O<sub>3</sub> in the PVA matrix electrolyte. Due to addition of filler, the amorphousness of the system increases

and different modes get weaken thereby peaks at 1406, 1317, 706, 619cm<sup>-1</sup> related to NH def. vib. CH def. vib. asym and C-H wagging mode..

Also, doublet peaks at 2942cm<sup>-1</sup> and 2920cm<sup>-1</sup> related to methyl C-H stretch in pristine gel electrolyte shift towards the lower wave number with broadness on addition of Al<sub>2</sub>O<sub>3</sub> filler in the PVA matrix electrolyte on account of salt-filler-polymer interaction. These variations recommends complex formation of PVA-NH<sub>4</sub>CH<sub>3</sub>COO and [PVA-NH<sub>4</sub>CH<sub>3</sub>COO:×wt%Al<sub>2</sub>O<sub>3</sub>] which have also been witnessed during XRD studies. It is evident that Al<sub>2</sub>O<sub>3</sub> acts as active filler in PVA matrix, which strongly modifies the morphology of the system.

**Table 2.** IR transmittance band (in wavenumbers) of Nanocomposite polymer gel membranes.

Description of Vibrations Mode	PVA	PVA-DMSO	NH <sub>4</sub> CH <sub>3</sub> COO	[(PVA-NH <sub>4</sub> CH <sub>3</sub> COO):Al <sub>2</sub> O <sub>3</sub> ] System			
				0.0wt%	0.2wt%	0.5wt%	1.0wt%
C H out of plane deformation	714	702	618 657	619 706	704.63	705	703
Sketletal C-H rocking mode	829	843		906	896.7	905	898
O-H bending mode	923	951		951	648.73	944	949
Out of plane N-H bending			922				
C-H wagging mode		1013	1014	1006	1010.95	1007	1012
C-O stretching mode	1083	1094	1046	1095	1099.05	1095	1095.5
C-C and C-O stretching mode of doubly	1135	1141		1139	1140.61	1146	1144
C-O stretching mode	1236		1244				
CHOH bending mode CH <sub>3</sub> in plane deformation	1326	1317		1317	1316	1315	1318
CH <sub>3</sub> bending mode			1338 1401				
N-H deformation and asymmetric CH <sub>3</sub> bending		1362 1375					
	1410	1406 1418		1406	1405	1406	1406
C-H deformation mode	1445	1436		1439	1437	1437	1435
N-H bending mode			1471 1539				
C-H stretching	1643			1650	1651	1662	1659
-CONH- bending mode	1661	1659					
C=O stretching mode			1734				
	2845						
C-H symmetric stretching mode of CH <sub>2</sub> group	2906 2937	2913 2939	2209 2790	2920 2942	2917 2944	2919 2941	2917 2942
	3059	3006	3008	3014	3013	3010	3014
O-H stretch	3295	3288	3210	3372	3362	3349	3559

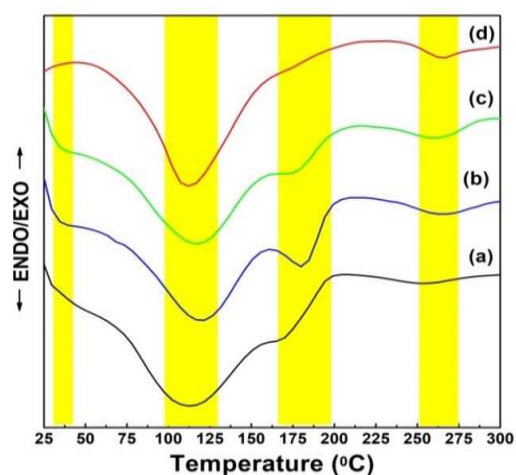


**Figure 4.** DSC thermogram of [PVA-NH<sub>4</sub>CH<sub>3</sub>COO:×wt% Al<sub>2</sub>O<sub>3</sub>] with (a) 0.0wt% (b) 0.2wt%, (c) 0.5wt% (d) 1.0wt% Al<sub>2</sub>O<sub>3</sub> nanoparticles doped NCPGE membranes.

### 3.4. Thermal Analysis

Polymeric materials typically reveal the presence of crystalline and amorphous phases. Such polymers exhibit melting transitions proportionate to their crystalline and glass transition for amorphous phases. PVA is one of such polymers which reveal T<sub>g</sub> closed to 80°C and melting transition T<sub>m</sub> around 200°C [12, 17]. Nanocomposite gel Polymer electrolytes are characterized as a liquid electrolyte fascinated within the microspores of polymer network, therefore, the thermal behavior of polymer is expected to be affected by the interaction between the components. Figure 4(a-d) shows the DSC thermogram represented the thermal scan for [PVA-NH<sub>4</sub>CH<sub>3</sub>COO:×wt%Al<sub>2</sub>O<sub>3</sub>] system for different filler (Al<sub>2</sub>O<sub>3</sub>) concentrations. Various thermal transitions noticed in the DSC pattern for NCPGEs under the study are shown in table 3.

The shift in glass transition temperature and melting temperature with composition (table 3) can be related to the



flexibility of polymeric backbone which intern affects conductivity behavior [12, 17-18].

**Table 3.** Temperature ( $^{\circ}\text{C}$ ) of transition in DSC thermograms of  $[\text{PVA-NH}_4\text{CH}_3\text{COO}:\times\text{wt}\%\text{Al}_2\text{O}_3]$  system in NCPGE membranes.

$[\text{PVA-NH}_4\text{CH}_3\text{COO}:\times\text{wt}\%\text{Al}_2\text{O}_3]$					
wt% $\text{Al}_2\text{O}_3$	$T_{g1}$	$T_{g2}$	$T_{g3}$	$T_{m1}$	$T_{m2}$
0.0	31.20	68.93	113.21	166.94	261.22
0.2	36.50	69.26	118.55	180.40	269.66
0.5	37.13	70.33	119.05	180.35	268.52
1.0	41.12	70.14	117.80	180.40	268.50

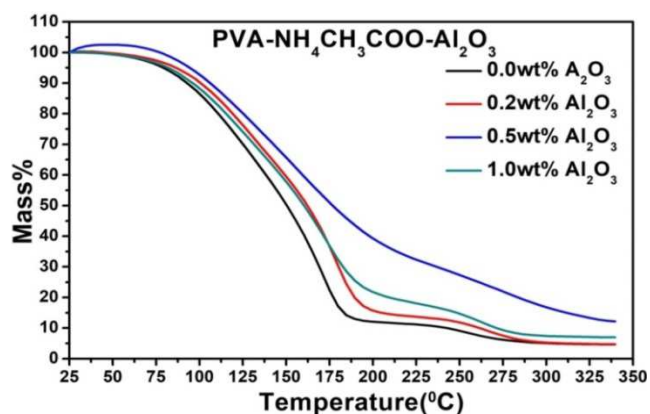
Close observation of DSC scans (figure 4) did not reveal any thermodynamics transition in the range  $195^{\circ}\text{C}$ - $250^{\circ}\text{C}$  related to melting transition of PVA of a system which reflects complete interaction of polymer component with salt leading to formation of new materials with improved thermal stability. This is observed from DSC scanning in nanocomposite polymer gel electrolyte samples follow a broad endothermic transition in the temperature range  $95^{\circ}\text{C}$ - $150^{\circ}\text{C}$ . The broadness in this transition can be linked to three factors, namely, evaporation of water formed during interaction of PVA and DMSO existence of melting transition of ammonium acetate salt ( $110^{\circ}\text{C}$ - $114^{\circ}\text{C}$ ) and presence of gel structure. Water formation during PVA-DMSO interaction has been previously reported by Agrawal and Awadhia [13, 19]. Because of such loosely bond water intercalated in ordered texture PVA, gel sample shows some phantom melting at relatively lower temperature around  $125^{\circ}\text{C}$  where detachment of such loosely bond water from gel texture takes place [20-22]. Thus such a transition is neither a glass transition nor a pure melting transition but some kind of gel-sol transition [19, 21]. It is further observed in thermogram of NCPGEs that a broad shoulder transition related to complex of polymer salt and filler appears in the temperature range ( $150^{\circ}\text{C}$ - $200^{\circ}\text{C}$ ). Broadness of this transition increases and the melting temperature of polymer electrolyte is observed (around  $167^{\circ}\text{C}$ ) shift towards higher temperature upon addition of  $\text{Al}_2\text{O}_3$  (scan b-d). This is probably due to improve interaction among polymer component in the presence of added salt and filler. Close examination of DSC profile (scan a) shows an endothermic transition in the temperature region around  $68^{\circ}\text{C}$  is known as glass transition of PVA (around  $90^{\circ}\text{C}$ ) which shift toward lower temperature due to interaction of PVA between salt and polymer [12, 13]. DSC profiles record a small endothermic transition in low temperature region ( $35^{\circ}\text{C}$ - $40^{\circ}\text{C}$ ) in all the scans which can be linked to attenuation of DMSO into DMS. The broad peak presence of the third endothermic transition in ( $250^{\circ}\text{C}$ - $275^{\circ}\text{C}$ ) reaffirm improvement in thermal stability of composite system with existence of amorphous nature on addition of  $\text{Al}_2\text{O}_3$  filler [17].

Figure 5 depicts the TGA thermograms of synthesized nanocomposite polymer gel electrolyte  $[\text{PVA-NH}_4\text{CH}_3\text{COO}:\times\text{wt}\%\text{Al}_2\text{O}_3]$  system for different filler concentration which illustrates three major weight losses and corresponding temperature region have been listed in table 4. The preliminary sluggish and little weight loss in the range ( $25^{\circ}\text{C}$ - $80^{\circ}\text{C}$ ) for all TGA curves can be related to removal of DMS.

**Table 4.** TGA data of  $[\text{PVA-NH}_4\text{CH}_3\text{COO}:\times\text{wt}\%\text{Al}_2\text{O}_3]$  system in NCPGE membranes.

$[\text{PVA-NH}_4\text{CH}_3\text{COO}:\times\text{wt}\%\text{Al}_2\text{O}_3]$ M*= mass loss						
wt% $\text{Al}_2\text{O}_3$	Region-I		Region-II		Region-III	
	$T_1(^{\circ}\text{C})$	M*%	$T_2(^{\circ}\text{C})$	M*%	$T_3(^{\circ}\text{C})$	M*%
0.0	25-75	3.48	75-180	75.53	180-300	14.35
0.2	25-75	3.65	75-195	74.83	195-300	11.26
0.5	25-75	3.45	25-190	72.13	190-300	9.75
1.0	25-80	3.55	80-200	70.72	200-300	9.56

The mass of nanocomposite polymer gel electrolyte decrease continuously with increase in the  $\text{Al}_2\text{O}_3$  nano filler in the second weight loss temperature range ( $75^{\circ}\text{C}$ - $200^{\circ}\text{C}$ ) is attributed to the evaporation of soaked water or rearrangement of intra and intermolecular hydrogen-bonded partially order texture. Decrease in loss appears to result from improve interaction of salt and polymer leading to improve thermal stability. TGA thermogram in temperature range ( $180^{\circ}\text{C}$ - $300^{\circ}\text{C}$ ) correlated to weight loss value are quite low which are related to decomposition of uncomplexed PVA in the system and thus too decreases with increases of  $\text{Al}_2\text{O}_3$  filler content.



**Figure 5.** TG thermogram of  $[\text{PVA-NH}_4\text{CH}_3\text{COO}:\times\text{wt}\%\text{Al}_2\text{O}_3]$  with different concentrations of  $\text{Al}_2\text{O}_3$  nanoparticles doped NCPGE membranes.

### 3.5. Cyclic Voltammetry Studies

Figure 6(a-d) shows the cyclic voltagrams for  $\text{Al}_2\text{O}_3$  soaked  $\text{PVA-NH}_4\text{CH}_3\text{COO}$  composite electrolytes system. On addition of 0.2wt%  $\text{Al}_2\text{O}_3$  filler (scan b), stability is seen to improve. A small oxidation peak appears at 0.5V in cyclic voltagram 'a' which corresponds to  $\text{NH}_4^+/\text{H}^+$  ion thereby indicating 98% protonic conduction in NCPGEs [12, 23]. Further, on increasing  $\text{Al}_2\text{O}_3$  contents, the oxidation peak (related to  $\text{NH}_4^+/\text{H}^+$ ) calculated by the  $t_{\text{ion}}$  studies shown in table 1 which tends to diminish and finally disappears in cyclic voltagrams figure 6(c & d). This feature ascertains change in system morphology subsequent to  $\text{Al}_2\text{O}_3$  insertion in pristine electrolyte matrix. Besides voltagram 'b' shows a small peak around 1.6V. This is possibly due to oxidation of  $\text{Al}_2\text{O}_3$  -a feature reported in past for  $\text{Ag}|\text{AgCl}$  (3M NaCl) in an aqueous 0.1 M KCl electrolyte solution [24-25]. Interestingly, this oxidation peak tends to reduce with increasing  $\text{Al}_2\text{O}_3$  filler contents in polymer gel electrolyte voltagrams figure 6(b & c). In comparison to  $[\text{PVA-NH}_4\text{CH}_3\text{COO}:\times\text{wt}\%\text{BiNiFeO}_3]$

NCPE, the improved cyclic stabilities of the  $[\text{PVA-NH}_4\text{CH}_3\text{COO}:\times\text{wt}\%\text{Al}_2\text{O}_3]$  NCPGE gel membrane was noticed [12, 26-27]. These anodic and cathodic peaks diminish in intensity and become broaden along with shifting of anodic peak towards higher potential and cathodic peak towards lower potential in each of the voltogram of NCPGEs in figure 6(b-d). This is essentially due to interaction of polymer with the  $\text{NH}_4\text{CH}_3\text{COO}$  salt in the presence of  $\text{Al}_2\text{O}_3$  nanofiller.

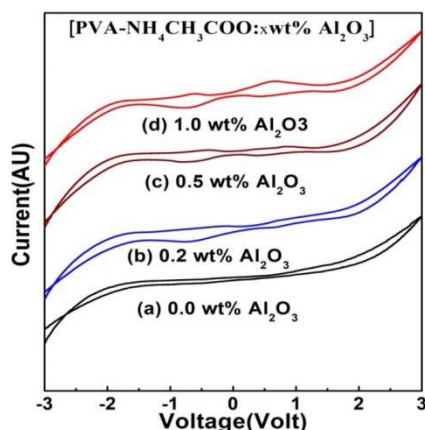


**Figure 6.** Cyclic voltammograms of (a) PVA: $\text{NH}_4\text{CH}_3\text{COO}$  gel membranes and its composites containing (b) 0.2 wt% (c) 0.5 wt% (d) 1.0 wt%  $\text{Al}_2\text{O}_3$  nanoparticles.

Similarly, the optimum operational potential energy for  $\text{Al}_2\text{O}_3$  doped NCPGE system examined by carrying out Linear Sweep Voltammetry (LSV) measurement (figure 7). In PVA- $\text{NH}_4\text{CH}_3\text{COO}$  system, the electrochemical window stability is expanded upto  $\pm 4.78\text{V}$  at 1.0wt%  $\text{Al}_2\text{O}_3$  soaked system (figure 7 inset image). The cathodic and anodic potentials are detected at  $-2.76\text{V}$  and  $+2.02\text{V}$  respectively. It can be concluded that infused of  $\text{Al}_2\text{O}_3$  can improve the electrochemical stability of the system.

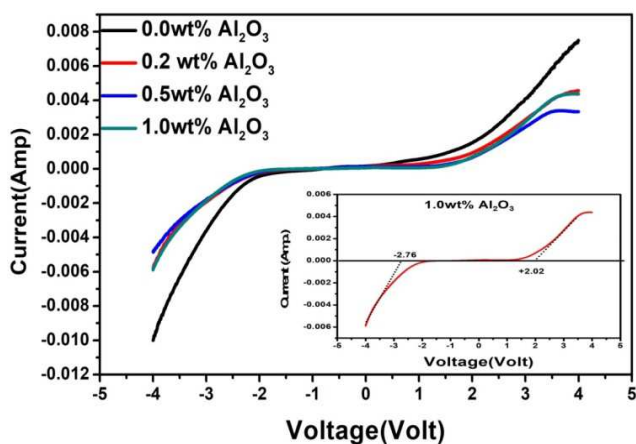


**Figure 7.** Linear Sweep Voltammetry (LSV) of  $[\text{PVA}:\text{NH}_4\text{CH}_3\text{COO}:\times\text{wt}\%\text{Al}_2\text{O}_3]$  system with varying concentrations of  $\text{Al}_2\text{O}_3$  nanoparticles.

### 3.6. Conductivity Studies

Figure 8 shows that the conductivity of NCPGE films improves slightly in magnitude till 0.5wt% and thereafter decreases till 0.8wt% before rising again (upto 1wt%) to reach

an optimum of  $\sigma_{\text{max}} = 3.88 \times 10^{-4} \text{ Scm}^{-1}$  and ultimately falling off beyond 1wt%  $\text{Al}_2\text{O}_3$  concentration in composite electrolyte. This feature is typically noticed earlier in the nanocomposite polymer electrolytes [12, 26]. XRD studies (figure 2) have shown intercalation of  $\text{Al}_2\text{O}_3$  with pristine electrolyte. This intercalation is likely to promote dissociation of salt leading to enhancement in the value of carrier concentration. Such a conclusion is envisaged on the fact that Lewis acid-base interactions between the heterogeneously dispersed filler surface and anions compete with interactions between cations and anions promoting salt dissociation via a sort of ion-filler complex formation. Thus at low filler concentration, greater dissociation of salt and increase in amorphous behavior (XRD studies) tends to enhance free ions concentration and mobility which significantly enhances ionic conductivity. The conductivity response beyond 0.5wt%  $\text{Al}_2\text{O}_3$  content can be associated to the fact that all the salt has been dissociated and so charge carrier concentration is limited. It is only the change in system morphology which tends to affect the conductivity. At higher concentration of nanofillers i.e. beyond 0.5wt% loading they serve as cross linking centres for polymer segments causing immovability of polymer chains in accordance with Tsagarapoulos model [14] and thereby dropping the conductivity of the system. The second conductivity maxima is related to formation of highly conducting interfacial layer between  $\text{Al}_2\text{O}_3$  and gel electrolyte caused by filler salt interaction and which dominates over ion pairing effect.

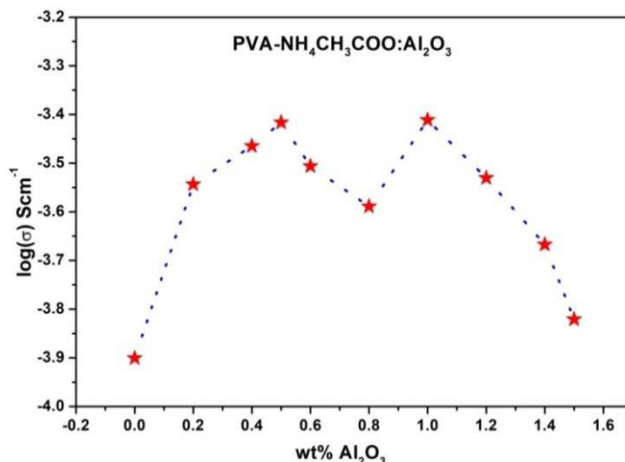


**Figure 8.** dc conductivity of nanocomposite polymer gel electrolyte membranes with varying concentrations of  $\text{Al}_2\text{O}_3$  nanofiller.

Further, Ranjta *et al* [27] have recently reported the effect of  $\text{BiNiFeO}_3$  nano particle variation on ionic conductivity of  $[\text{PVA-NH}_4\text{CH}_3\text{COO}:\times\text{wt}\%\text{BiNiFeO}_3]$  gel electrolytes. They have shown that complex formation takes place in the system, which tends to raise the conductivity of the system through greater dissociation of salts in the presence of filler [27]. Here, it is worthwhile to mention that as filler content increases beyond 1wt%, films become brittle. Thus it is concluded that upper limit for favorable absorption of filler in the case of  $[\text{PVA-NH}_4\text{CH}_3\text{COO}:\times\text{wt}\%\text{Al}_2\text{O}_3]$  system is 1wt%. Because morphology of films are directly linked to mobility of charge

carrier to migrate upon application of electric field, ionic conductivity of polymer electrolytes is bound to be influenced by the morphology of system. The temperature dependence of the electrical conductivity of the polymer gel electrolyte and its composite membranes is presented in figure 9. The increase in conductivity with temperature is attributed to hopping mechanism between coordinated sites, local structural relaxation and segmental motion of the polymer. As the amorphous region progressively increases, the polymer chain acquires faster internal motion and bond rotations (segmental motions). This in turn favors the hopping of inter-chain and intra-chain movement and ionic conductivity of polymer electrolyte becomes high.

It is apparent from conductivity behavior (figure 9) that all the curves show two linear regions separated by a nonlinear behavior. The linear region in the low temperature region (38°C to 60°C), conductivity obeys Arrhenius nature as described earlier [12, 27]. This is possibly due to presence of liquid electrolyte encapsulated by the polymer matrix i.e. effect of temperature of conductivity of liquid electrolytes. The high temperature regime (50°C to 90°C) conductivity response can be well described by VTF relationship. Therefore, all the curves display similar behavior i.e. a combination of Arrhenius and VTF character.

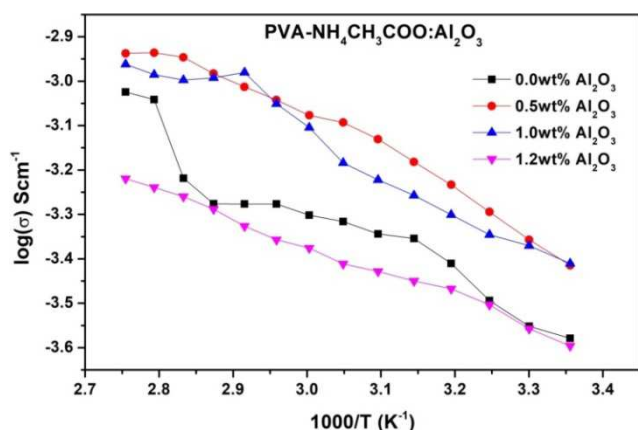


**Figure 9.** Variation of temperature dependence ionic conductivity of [PVA-NH<sub>4</sub>CH<sub>3</sub>COO:xwt% Al<sub>2</sub>O<sub>3</sub>] nanocomposite polymer gel electrolytes membranes with 0.0, 0.5, 1.0 & 1.2 wt% concentrations of Al<sub>2</sub>O<sub>3</sub> nanoparticles.

## 4. Conclusion

Nanocomposite polymer gel electrolytes (NCPGEs) based on PVA dispersed with Al<sub>2</sub>O<sub>3</sub> filler have been successfully synthesized by solution cast technique. XRD studies reveal that the amorphicity enhanced by admixing nanosized Al<sub>2</sub>O<sub>3</sub> filler. Further, low degree of crystallinity reflects high amorphous nature of composite polymeric gels. The complexation between polymer and salt has been observed in X-ray analysis. The SEM images show heterogeneous distribution of fillers in nanocomposite electrolyte system and chains of PVA fully covered with Al<sub>2</sub>O<sub>3</sub> filler. FTIR spectral studies have established the Al<sub>2</sub>O<sub>3</sub> serves the role of active filler and causing structural changes in the system. DSC

studies show improvement in thermal behavior of the system subsequent to filler particles addition. Cyclic voltametric investigations show that electrochemical window extends from -2.76V for pristine electrolyte to +2.02V for NCPGEs. Bulk ionic conductivity has been found to increase steadily with increasing Al<sub>2</sub>O<sub>3</sub> content and optimum at 1M salt concentration enhances upto 1wt% Al<sub>2</sub>O<sub>3</sub> filled nanocomposite electrolyte ( $\sigma_{\max}=3.88 \times 10^{-4} \text{ Scm}^{-1}$ ). Temperature dependent study of bulk conductivity response is described by the combination of Arrhenius and VTF behaviors. Wide electrochemical stability of  $\pm 4.78\text{V}$  is achieved on addition of 1wt% Al<sub>2</sub>O<sub>3</sub> filler and shows the presence of proton H<sup>+</sup> ion in the system suitable for the development of environment friendly rechargeable proton-conducting batteries application.

## Acknowledgements

Authors are grateful to the Department of Physics, Pt. Ravishankar Shukla University, Raipur (C.G.) for providing XRD analysis and performing DSC/TGA characterizations from Department of Physics, Dr. Hari Singh Gour University, Sagar (M.P.).

## References

- [1] Verma, M. L., Minakshi, M., & Singh, N. K. (2014). Synthesis & characterization of solid polymer electrolyte based on activated carbon for solid state capacitor. *Electrochimica Acta*, 137, 497-503. doi: 10.1016/j.electacta.2014.06.039.
- [2] Zhou, D., Shanmukaraj, D., Tkacheva, A., Armand, M., & Wang, G. (2019). Polymer Electrolytes for Lithium-Based Batteries: Advances and Prospects. *Chem*, 5 (9), 2326-2352. doi: <https://doi.org/10.1016/j.chempr.2019.05.009>.
- [3] Cheng, X., Pan, J., Zhao, Y., & Liao, M. (2017). Gel Polymer Electrolytes for Electrochemical Energy Storage. *Advanced Energy Materials*, 8 (7): 1702184. doi: 10.1002/aenm.201702184.
- [4] Wen, P., Zhao, Y., Wang, Z., Lin, J., Chen, M., & Lin, X. (2021). Solvent-Free Synthesis of the Polymer Electrolyte via Photo-Controlled Radical Polymerization: Toward Ultrafast In-Built Fabrication of Solid-State Batteries under Visible Light. *ACS Applied Materials And Interfaces*, 13 (7), 8426-8434. doi: <https://doi.org/10.1021/acsami.0c21461>.
- [5] Jeon, J. K., Kwak, S. Y., & Cho, B. W. (2005). Solvent-Free Polymer Electrolytes. *Journal Of The Electrochemical Society*, 152 (8), 1583-1589. doi: 10.1149/1.1939167.
- [6] Kumar, K. N., Vijayalakshmi, L., & Ratnakaram, Y. C. (2015). Energy transfer based photoluminescence properties of (Sm<sup>3+</sup> + Eu<sup>3+</sup>): PEO+PVP polymer films for red luminescent display device applications. *Optical Materials*, 45, 148-155. doi: 10.1016/J.OPMAT.2015.03.025.
- [7] Eltoun, M. S. A., Nasr, R. M. O., & Omer, H. M. A. (2020). Preparation and characterization of CuO nanoparticles using sol-gel method and its application as CuO/Al<sub>2</sub>O<sub>3</sub>. *American Journal of Nano Research and applications*, 8 (2), 16-21. doi: 10.11648/j.nano.20200802.

- [8] Wu, H. D., Wu, I. D., & Chang, F. C. (2001). The interaction behavior of polymer electrolytes composed of poly (vinyl pyrrolidone) and lithium perchlorate (LiClO<sub>4</sub>). *Polymer*, 42 (2), 555-562. doi.org/10.1016/S0032-3861(00)00213-5.
- [9] Song, M. K., Kim, Y. T., & Tae, Y. (2003). Thermally Stable Gel Polymer Electrolytes. *Journal of The Electrochemical Society*, 150 (4), 439-444. doi: 10.1149/1.1556592.
- [10] Huy, V. P. H., So, S., & Hur J. (2021). Inorganic Fillers in Composite Gel Polymer Electrolytes for High-Performance Lithium and Non-Lithium Polymer Batteries. *Nanomaterials*, 11 (3), 614. doi: 10.3390/nano11030614.
- [11] Stephan, A. M., & Nahm, K. S. (2006). Review on composite polymer electrolytes for lithium batteries. *Polymer*, 47 (16), 5952-5964. doi: 10.1016/j.polymer.2006.05.069.
- [12] Chand, N., Rai, N., Agrawal, S. L., & Patel, S. K. (2011). Morphology, thermal, electrical and electrochemical stability of nano aluminium-oxide-filled polyvinyl alcohol composite gel electrolyte. *Bulletin Of Material Science*, 34 (7), 1297-1304. doi: 10.1007/s12034-011-0318-7.
- [13] Awadhia, A., & Agrawal, S. L. (2007). Structural, thermal and electrical characterizations of PVA:DMSO:NH<sub>4</sub>SCN gel electrolytes. *Solid State Ionics*, 178 (13-14), 951-958. doi: 10.1016/j.ssi.2007.04.001.
- [14] Agrawal, S. L., Rai, N., Natarajan, T. S., & Chand, N. (2013). Electrical characterization of PVA-based nanocomposite electrolyte nanofibre mats doped with a multiwalled carbon nanotube. *Ionics*, 19, 145-154. doi: 10.1007/s11581-012-0713-0.
- [15] Deepa, M., Sharma, N., Agnihotry, S. A., & Chandra, R. (2002). FTIR investigations on ion-ion interactions in liquid and gel polymeric electrolytes: LiCF<sub>3</sub>SO<sub>3</sub>-PC-PMMA. *Journal Of Materials Science*, 37, 1759-1765. doi: 10.1023/A:1014921101649.
- [16] Ghezlbash, Z., Ashouri, D., Mousavian, S., Ghandi, A. H., & Rahnama, Y. (2012). Surface modified Al<sub>2</sub>O<sub>3</sub> in fluorinated polyimide/Al<sub>2</sub>O<sub>3</sub> nanoparticles: Synthesis and characterization. *Bulletin Of Materials Science*, 35, 925-931. doi: 10.1007/s12034-012-0385-4.
- [17] Chand, N., Rai, N., Natarajan, T. S., & Agrawal, S. L. (2011). Fabrication and Characterization of nano Al<sub>2</sub>O<sub>3</sub> filled PVA: NH<sub>4</sub>SCN Electrolyte Nanofibers by Electrospinning. *Fibers and Polymers*, 12 (4), 438-443. doi: https://doi.org/10.1007/s12221-011-0438-0.
- [18] Agrawal, S. L., & Shukla, P. K. (2000). Structural and electrical characterization of polymeric electrolytes: PVA-NH<sub>4</sub>SCN system. *Indian Journal Of Pure And Applied Physics*, 38, 53-61.
- [19] Agrawal, S. L., & Awadhia, A. (2004). DSC and conductivity studies on PVA based proton conducting gel electrolytes. *Bulletin of Materials Science*, 27, 523-527. doi: 10.1007/BF02707280.
- [20] Mukherjee, G. S., Shukla, N., Singh, R. K., & Mathur, G. N. (2004). Studies on the properties of carboxymethylated polyvinyl alcohol. *Journal Of Scientific And Industrial Research*, 63, 596-602.
- [21] Dibbern, D. B., & Atvars, T. D. Z. (2000). Thermal transitions of poly(vinyl alcohol) hydrogel sensed by a fluorescent probe. *Journal Of Applied Polymer Science*, 75 (6), 815-824. doi: 10.1002/(SICI)1097-4628(20000207)75:6<815:AID-APP11>3.0.CO;2-0.
- [22] Zou, G. X., Jin, P. Q., & Xin, L. Z. (2008). Extruded Starch/PVA Composites: Water Resistance, Thermal Properties, and Morphology. *Journal Of Elastomers and Plastics*, 40, 303-316. doi: 10.1177/0095244307085787.
- [23] Sharma, S., Dhiman, N., Pathak, D., & Kumar, R. (2016). Effect of Donor Number of Plasticizers on Conductivity of Polymer Electrolytes Containing NH<sub>4</sub>F. *i-Manager's Journal On Material Science*, 3 (4), 28-34. doi: 10.26634/jms.3.4.4825.
- [24] Ito, T., Sun, L., & Crooks, R. M. (2003). Electrochemical Etching of Individual Multiwall Carbon Nanotubes. *Electrochemical And Solid-State Letters* 6 (1), C4-C7.
- [25] Hinds, B. J., Chopra, N., Rantell, T., Andrews, R., Gavalas, V., & Bachas, L. G. (2004). Aligned Multiwalled Carbon Nanotube Membranes. *Science*, 303, 62-65. doi: 10.1126/science.1092048.
- [26] Haque, M. A., Sulong, A. B., Shyuan, L. K., Majlan, E. H., Husaini, T., & Rosli, R. E. (2021). Synthesis of polymer/MWCNT nanocomposite catalyst supporting materials for high-temperature PEM fuel cells. *International Journal of Hydrogen Energy*, 46 (5) 4339-4353. doi: 10.1016/j.ijhydene.2020.10.223.
- [27] Ranjta, L., Singh, C. P., & Rai, N. (2022). Experimental investigations on nano-ferrite embedded nanocomposite polymer electrolytes for proton-conducting rechargeable batteries application. *Materials Today: Proceedings*, 54 (3), 702-709. doi: 10.1016/j.matpr.2021.10.408.